JOURNAL OF CATALYSIS 30, 235–249 (1973)

Decomposition of Formic Acid on Ni(110)

I. Flash Decomposition from the Clean Surface and Flash Desorption of Reaction Products

JON McCARTY, JOHN FALCONER, AND ROBERT J. MADIX

Department of Chemical Engineering, Stanford University, Stanford, California 94305

Received February 5, 1973

The flash decomposition of adsorbed formic acid on clean Ni⟨110⟩ produced H_2O, CO, H_2, and CO_2 peaks. The CO decomposition peak appeared at much higher temperatures than the H_2 or CO_2 decomposition peaks; it was identical to the flash desorption peak of adsorbed CO. The H_2O peak was observed at temperatures well below the H_2 and CO_2 decomposition peaks. The H_2 and CO_2 decomposition peaks were identical and quite narrow. The insensitivity of the peak temperature of H_2 and CO_2 to initial coverage and the detailed peak shapes were inexplicable by simple mechanisms; they were suggestive of an autocatalytic decomposition. The hydrogen decomposition peak occurred at a much higher temperature than the flash desorption peak of H_2.

The initial sticking probability of formic acid was near unity at room temperature. Low exposures to formic acid produced CO and surface oxidation. The sticking probability of H_2 was quite temperature sensitive, increasing from 0.01 to 0.5 between 50 and $-25°C$; it was immeasurable on a carbon-covered surface. The initial sticking probability of CO was 0.7 ± 0.2. Decomposition of CO_2 to adsorbed CO and O occurred with a probability of 0.15 per incident CO_2 molecule.

INTRODUCTION

The interaction of formic acid with a clean ⟨110⟩ nickel single crystal surface was studied in an ultra high vacuum system. The objective of this study was to obtain kinetic information about the catalytic decomposition of formic acid on the clean surface and to determine how surface impurities of carbon, sulfur, and oxygen, as well as surface structure, effect the kinetics of this reaction. Results on contaminated surfaces will be presented in a later paper. Experiments employing a combination of mass spectrometric flash desorption, Auger spectroscopy, and LEED are reported below.

The decomposition of formic acid on metals and metal oxide surfaces has been extensively studied by many workers. In most cases the reaction was studied in batch, flow or recirculating reactors at relatively high pressures (10^{-5}–100 Torr). Also the surfaces used were usually not well defined in terms of surface structure and composition (powders, decomposed formates, or carbonates). Recent advances in analytical techniques such as Auger electron spectroscopy (AES) for observing surface composition and structure make more detailed studies possible.

In general the observed reaction kinetics for this reaction is fairly simple, and the products can be readily separated and detected. Reasonable reaction rates occur at low temperatures, and since many materials catalyze the dehydrogenation reaction, it has been used as a test reaction for a large number of catalysts. The reaction, therefore, appeared particularly suitable for fundamental study on well characterized surfaces.

The three reaction paths for the decomposition are:

$$HCOOH \rightarrow H_2 + CO_2 \quad (1)$$
$$HCOOH \rightarrow H_2O + CO \quad (2)$$
$$2HCOOH \rightarrow H_2O + CO_2 + CH_2O. \quad (3)$$

Reaction (3) is not observed on metals (*1*), and the dehydrogenation reaction (1) is generally considered to be the major reaction on metal catalysts. The dehydration reaction usually occurs to less than one percent on nickel (*3–8*). One exceptional observation to this general pattern was due to Inglis and Taylor (*2*) who observed a large CO to CO_2 product ratio for decomposition on freshly deposited thin films of several metals ($CO/CO_2 = 0.41$ for nickel). After several experimental runs on a given film, however, they observed a large decrease in the CO/CO_2 ratio and obtained results similar to those for metal powders. They attributed this change in decomposition product ratio to surface contamination. In this study kinetic information on a clean surface was obtained by making use of Auger electron spectroscopy (AES) to monitor surface composition.

Experimental Methods

A stainless steel ultra high vacuum chamber was used as the flash desorption chamber (designed for use as a modulated molecular beam system). It was pumped by a 2000 liter/sec TSP and a 240 liter/sec Noble Vac Ion pump. After a twelve hour bake-out to 200°C for the chamber and 300°C for the shielded ion pump base pressures less than 5×10^{-10} Torr were reached routinely. The system contained PHI four grid LEED-Auger optics, an EAI quadrupole mass spectrometer, an argon ion bombardment gun, and a molecular beam source region. A schematic diagram of the apparatus is shown in Fig. 1.

A 0.05 mm thick nickel ⟨110⟩ single-crystal with 0.5 cm^2 area on each side was used. It was spotwelded to a 0.25 mm diameter nickel wire which was clamped to an alumina rod for electrical isolation. The crystal holder was connected to a linear rotary-motion feed-through located on top of the vacuum chamber. The sample could be heated linearly with time by either radiation or electron bombardment from a tungsten filament located 4 mm behind it. The thin sample could be cooled to −60°C by conduction through the alumina rod which was in thermal contact with a liquid-nitrogen cooling tube. After a typical flash to 500°C, the sample cooled back below room temperature in approximately two minutes. The total exposure to background gases between the completion of a flash

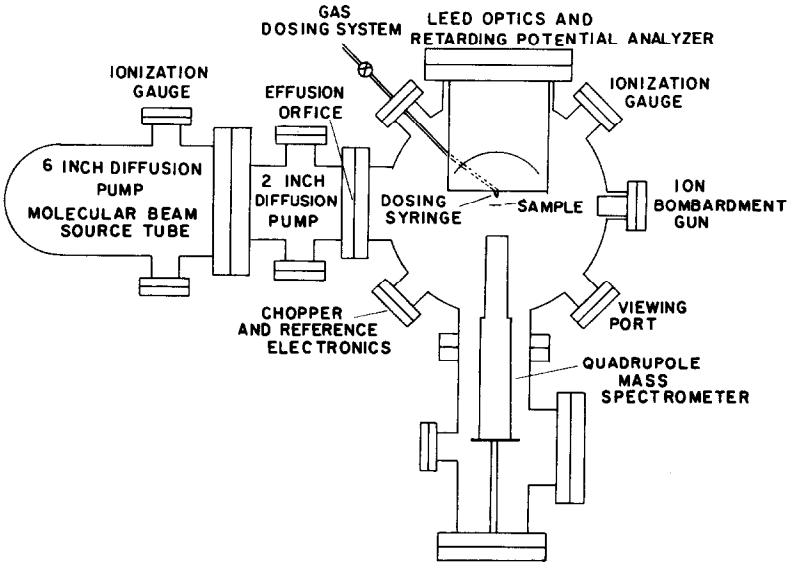

Fig. 1. Top view of ultra high vacuum flash desorption chamber.

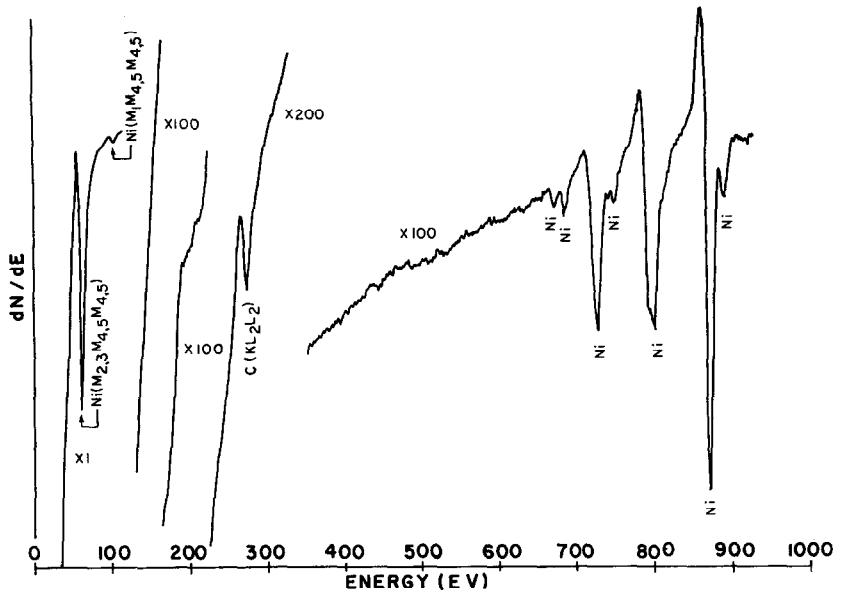

FIG. 2. Auger spectrum of "clean" Ni⟨110⟩ sample (2 kV gun voltage, 3.5 V r.m.s. modulation).

desorption and the start of the next adsorption sequence was negligible. The temperature of the crystal was measured by a chromel-alumel thermocouple spotwelded between the crystal and support wire.

The degree of surface contamination was monitored by Auger electron spectroscopy. An electron gun was suspended from the top of the chamber at an angle of 15° to the crystal plane and provided more than 100 μA of ionizing current at 2 kV. The retarding grid method was used to analyze the Auger electron current, and the lower limits of detection due to instrumental noise were estimated to be 2% of a surface layer for carbon and sulfur and less than 5% for oxygen. A typical "clean" Auger spectrum is shown in Fig. 2. This clean surface was obtained by argon ion sputtering and heating. All contaminants except carbon were readily removed by a typical cleaning cycle of 4×10^{-5} amps of Ar^+ ions at 300 V for 20 min followed by a brief anneal at 500°C. In the early stages of this work a sulfur peak and peaks at 165 and 180 V appeared upon heating to 750°C or after repeatedly flashing to 500°C (see Fig. 3). After many cleaning cycles and flashes, the sample could be heated to 750°C without any appearance of these Auger peaks; apparently the repeated cleaning and flashing cycles purified the bulk sufficiently to maintain a clean surface during flashing. All results reported below were obtained on these clean surfaces. Carbon was very difficult to remove

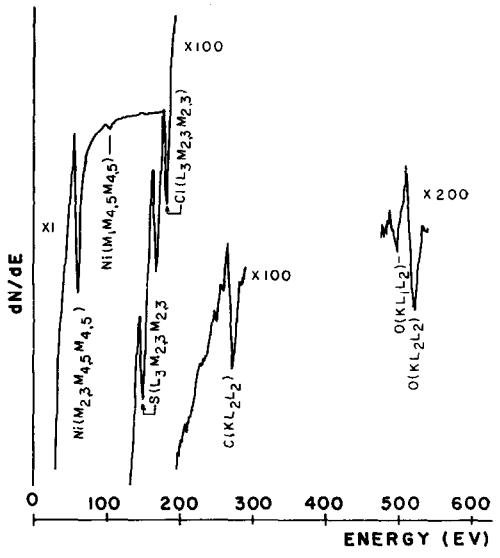

FIG. 3. Auger spectrum of Ni⟨110⟩ with contamination peaks due to numerous flashes to 500°C.

completely and a small amount was always present after Ar^+ sputtering. This level of surface carbon could be further reduced but not eliminated by heating the sample to about 500°C for several minutes. Usually less than 10% of a surface carbon monolayer resulted after this heating. A surface carbon monolayer was defined as the saturation carbon coverage (C_{et}) obtained from cracking ethylene at saturation coverage on the nickel surface. In fact, no difference in the desorption kinetics for HCOOH was observed when the carbon level was between 2 and 10% C_{et}. When carbon and/or oxygen built up on the surface due to carbon dioxide or formic acid exposure, a flash to 750°C eliminated oxygen and decreased the carbon to less than 0.1 C_{et}.

In order to minimize adsorption and decomposition of formic acid on the chamber walls the formic acid was introduced through a stainless steel syringe located in front of the LEED grids and directed at the front face of the crystal (see Fig. 1). During dosage the background pressure did not rise above 1×10^{-9} Torr, and the sample was dosed at an effective pressure greater than 3×10^{-8} Torr. Thus, as verified experimentally, negligible adsorption occurred on the back side of the sample during formic acid dosing. Product gases were adsorbed both through the doser or from ambient gas. In all cases the chamber was pumped below 1×10^{-9} Torr before the sample was flashed.

The formic acid (Baker and Admason reagent grade, 99.5% minimum assay, 0.40% maximum acetic acid impurity) was purified by repeated fractional crystallization until a constant freezing point of 8.4°C was reached. It was then twice vacuum distilled. This purification procedure left residual methanol and acetic acid, since fragments of mass numbers 31, 32, 43, and 60 were detected in the mass spectrum of the formic acid vapor. These impurities were completely removed by extended vacuum evaporation at −45°C. The formic acid vapor above the solid at −45°C was used to dose to sample. When not in use the formic acid was stored under vacuum in a dry ice–acetone bath. The composition of the gases used for adsorption studies were as follows; (a) hydrogen, Matheson ultrapure 99.999%, (b) argon, Matheson 99.995%, (c) carbon monoxide, Matheson Research Purity 99.99%, and (d) carbon dioxide, Liquid Carbonic U.S.P. grade 99.9%.

The flash desorption technique was used to study the adsorption and desorption of product gases as well as the adsorption and decomposition of formic acid. The results reported below were obtained using radiation heating from the tungsten filament located behind the sample in order to avoid the complications introduced by decomposing adsorbed formic acid by electron bombardment heating. Nearly linear flash rates up to 12°C/sec were used. The quadrupole mass spectrometer with a Brink-type axial ionizer functioned as a partial pressure indicator and was calibrated with a Bayard Alpert ionization gauge. The mass spectrometer signal was amplified by a Keithly electrometer and plotted on a X–Y recorder against the thermocouple voltage. Pumping speeds were measured frequently against known effusion rates through an orifice from the beam chamber, and they agreed well with values obtained from known leak rates through the dosing syringe.

LEED was used to verify the presence of the nickel ⟨110⟩ face and to observe the effect of formic acid adsorption. Preliminary results indicate no fractional order spots but some change in intensity of substrate spots was observed. More extensive LEED studies are in progress.

Results

A. Adsorption and Desorption of Hydrogen

Hydrogen was adsorbed on the Ni ⟨110⟩ surface from −55 to 55°C at pressures up to 1×10^{-7} Torr. Figures 4–6 show typical hydrogen desorption for adsorption at 25, 0, and −30°C, respectively. For adsorption at 25°C and above only one flash peak was found, the maximum desorption rate occurring around 80°C (peak temperature)

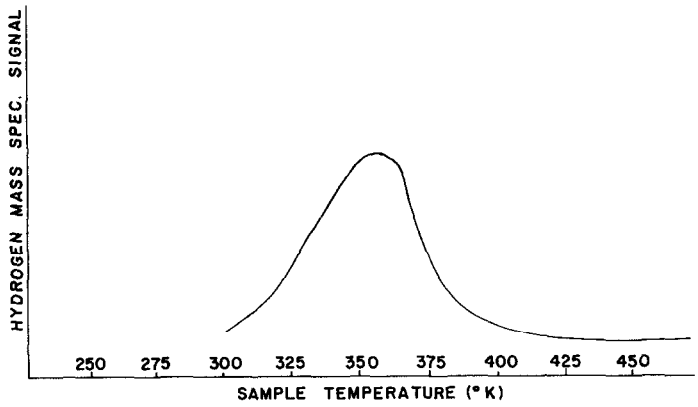

FIG. 4. Hydrogen flash desorption after 20 Langmuir hydrogen exposure at 25°C.

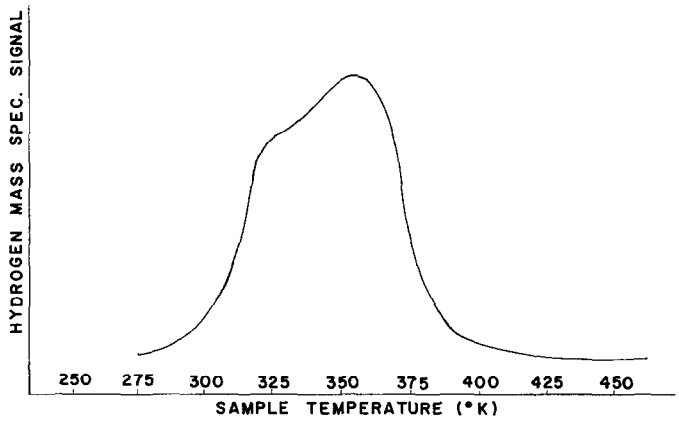

FIG. 5. Hydrogen flash desorption after 4 Langmuir hydrogen exposure at 0°C.

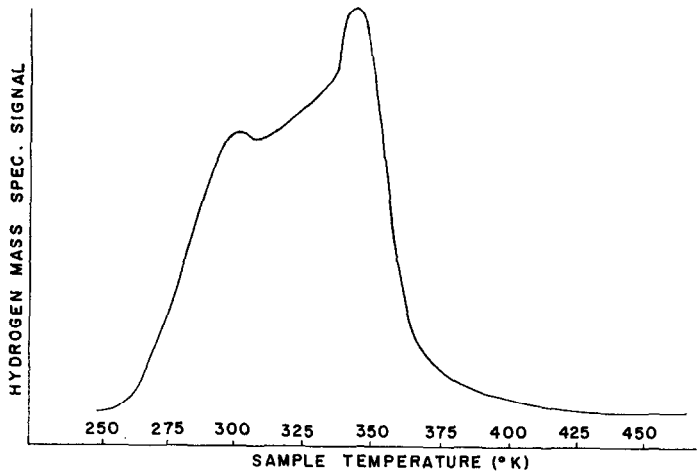

FIG. 6. Hydrogen flash desorption after 8 Langmuir hydrogen exposure at −30°C.

for a heating rate of 10°C/sec. The peak shape was symmetrical about the peak temperature indicating second order desorption kinetics. At lower temperatures, two desorption peaks were observed as seen in Fig. 6. The coverage for adsorption at 50°C reached a limiting valuc of 1.3×10^{14} molecules/cm^2.

Full coverage for adsorption at −25°C was approximately 4×10^{14} molecules/cm^2 with a sticking probability of 0.5 at coverages less than 1×10^{14} molecules/cm^2. Though the initial sticking probability at −25°C was 0.5 for the clean surface, at −25°C with a carbon coverage of 1.0 C_{et} no observable adsorption occurred after 100 Langmuirs exposure to hydrogen.

Figure 7 shows a plot of the natural logarithm of rate divided by the square of the coverage versus inverse temperature. A linear least-squares fit provided an activation energy of 25 kcal/g-mole and a pre-exponential factor of 1 cm^2/atom-sec. If the pre-exponential factor was taken to be 10^{-1} (a value typical of second-order surface reaction), the resulting activation energy was 23.5 kcal/g-mole. After several

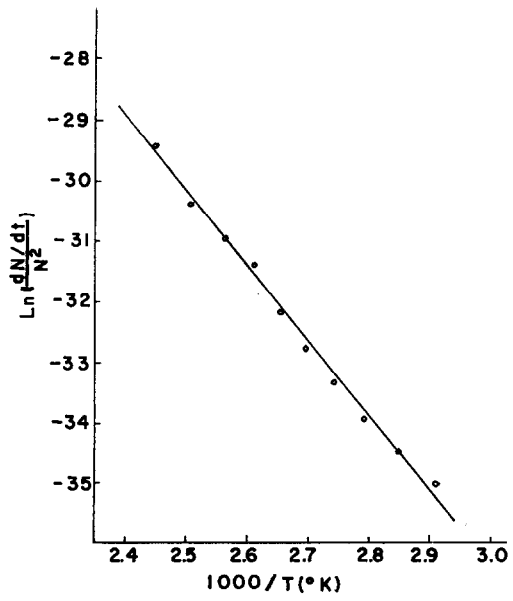

FIG. 7. Logarithm of ratio of desorption rate to square of coverage versus inverse temperature for hydrogen desorption after hydrogen exposure.

hydrogen flash desorption sequences the Auger electron spectrum remained essentially the same as before adsorption.

B. Adsorption and Desorption of Carbon Monoxide

Carbon monoxide readily adsorbed on Ni ⟨110⟩ at temperatures between −55 and 50°C at less than 10^{-8} Torr of CO pressure. The sticking probability at coverages less than 0.3 L exposure was 0.7 ± .2. Maximum coverage corresponded to 4×10^{14} molecules/cm^2.

A typical CO flash spectrum is shown in Fig. 8. Only one desorption peak was detected following CO adsorption at 35°C and flashing to 750°C. The peak occurred at 165°C ± 5°C, and the peak shape indicated first order desorption. An activation energy of 26 kcal/mole was obtained from the peak temperature (*9*) using a pre-exponential factor of 10^{13} sec^{-1}.

Exposure of the surface to greater than two Langmuirs of CO resulted in the appearance of a second small peak at 125°C ± 10°C, which appeared as a broadening on the low-temperature side of the 165°C peak. It had only 10% of the area of the peak at 165°C.

Exposing the surface to oxygen or bombarding adsorbed CO with the Auger electron beam produced two additional CO desorption peaks. These higher temperature peaks occurred at 380–410°C and 530–650°C. These peaks did not appear following CO adsorption on a clean surface. The sample was held at 200°C while the Auger spectrum was taken to minimize cracking adsorbed CO with the electron beam. After a series of CO adsorption and desorption cycles, the carbon coverage increased from 0.1 to 0.2 C_{et} but no oxygen was detected on the surface.

C. Adsorption of Carbon Dioxide

No carbon dioxide was observed to desorb from Ni ⟨110⟩ after exposure of 80 Langmuir at 25°C or 10 Langmuir at −55°C. Although no carbon dioxide was desorbed upon flashing, carbon monoxide was always detected after carbon dioxide exposure. Two experiments indicated that the CO flash

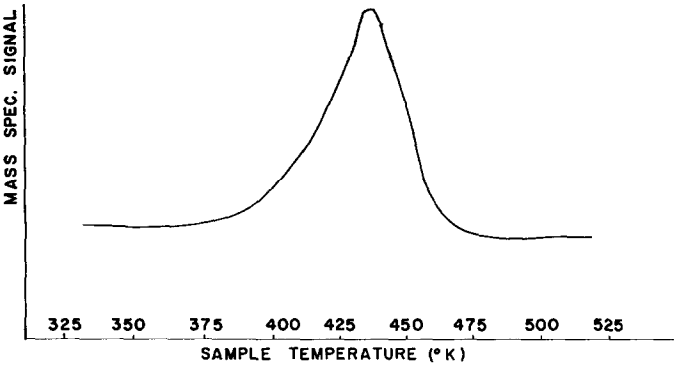

FIG. 8. Carbon monoxide flash desorption after 0.4 Langmuir carbon monoxide exposure at 45°C.

peak was not due to background CO; (a) CO_2 dosing through the syringe with the sample moved out of the way of the doser resulted in negligible CO desorption, and (b) CO flash desorption did not cause a buildup of oxygen on the surface, as was observed for CO_2 exposure.

The CO flash peaks following CO_2 adsorption were similar to the CO peaks arising from CO adsorption. The adsorption of CO_2 alone increased significantly the amount of surface oxygen after flashing the exposed surface to 500°C. The sticking probability of CO_2 to produce adsorbed CO was 0.15. The CO coverage observed for CO_2 exposure of 4.3 Langmuir was 1.8×10^{14} molecules/cm^2. The sticking probability was of the order of 0.1 for the clean surface or a slightly oxygenated surface.

D. Flash Decomposition of Formic Acid

Formic acid readily adsorbed on the Ni ⟨110⟩ surface at adsorption temperatures from −55°C to 80°C. The sticking probability for less than 0.2 Langmuir exposure was 0.9 ± .2 at 40°C. Formic acid did not desorb directly from the surface, and the only reaction products observed were H_2, CO_2, and CO.* At adsorption temperatures between 0 and 80°C carbon dioxide and hydrogen always desorbed in a single, very narrow peak when flashed. The temperatures corresponding to the maximum in the CO_2 and H_2 flash peaks were identical; they were always greater than the temperature corresponding to the peak for the desorption of adsorbed hydrogen. Except for height differences due to different pumping speeds and mass spectrometric sensitivities the flash peaks for products H_2 and CO_2 were nearly identical. The ratio of CO_2 to H_2 evolved was estimated to be 1.0 ± 0.2 in all instances. Immediately after formic acid flashes, AES showed a carbon decrease and an oxygen buildup on the surface (see Fig. 9). In all flashes the final flash temperature was 500°C; flashes to 500°C without gas adsorption resulted in a carbon increase and no detectable oxygen buildup. The carbon Auger signal was often reduced to the noise level by repeated formic acid flashes.

Typical flash spectra for CO_2, H_2 and CO from adsorbed formic acid are shown in Fig. 10 for adsorption at 50°C. The CO_2 and H_2 peaks were extremely narrow with a width at half maximum of 6.5 ± 0.5°C. The temperature at the peak maximum was 115° ± 0.5°C for a flash rate of 10°C/sec. The peaks were asymmetric about the maximum; the rate fell off more rapidly above the peak temperature than it rose below. Assuming the CO_2 flash desorption is described by a single first order rate limiting step, the Arrhenius rate constant required to produce such a sharp peak has an acti-

* Note added in proof: Recently we have observed H_2O from flashes following adsorption of formic acid below −30°C. Water itself shows two separate flash peaks, one below 0°C, and one at 100°C, indicating that H_2O may form upon the adsorption of formic acid at room temperature and above, but most of it is desorbed prior to the flash.

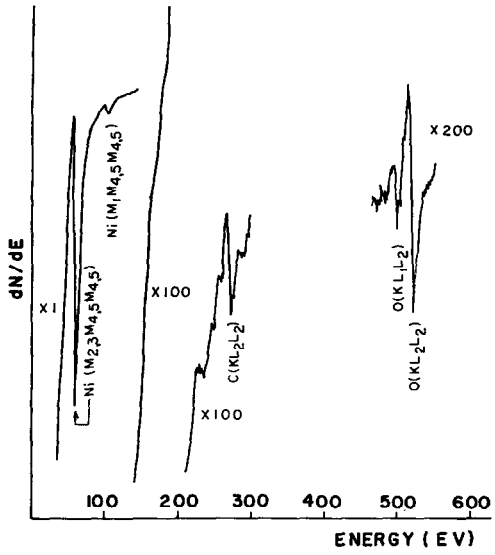

FIG. 9. Auger spectra of Ni⟨110⟩ after series of formic acid exposures and flashes to 500°C.

vation energy of 100 kcal/g-mole and a pre-exponential factor of 10^{60} sec^{-1} (see Discussion)!

The activation energy for first order desorption kinetics was also determined by changing the heating rate and noting the shift in peak temperature (*9*). In this case no assumption was made about the pre-exponential factor. Varying the flash heating rate from 2.1 to 25°C/sec produced a shift of 20°C in the peak temperature. Such a shift corresponded to an activation energy of 25 ± 5 kcal/g-mole.

Carbon monoxide also desorbed from the surface after exposure to formic acid, and a typical flash spectrum after adsorption at 50°C is also shown in Fig. 10. The narrow part of the low temperature peak had the same peak temperature and shape as the H_2 and CO_2 flash peaks. When the fraction of CO^+ ions due to cracking in the mass spectrometer ionizer was subtracted from the low temperature peak, a small peak remained at 100°C with an area 20–30% of the high-temperature CO area. The higher-temperature CO peak at 165°C was identical to the peak found for desorption of adsorbed CO and was located at the same temperature. The saturation CO peak observed with formic acid adsorption was 1.8×10^{14} molecules/cm², 40% of the maximum found for CO adsorption. The amount of CO desorbed at 165°C reached a limiting value at lower exposures than the CO_2 and H_2 peaks, as shown in Fig. 11.

In order to determine the extent of ad-

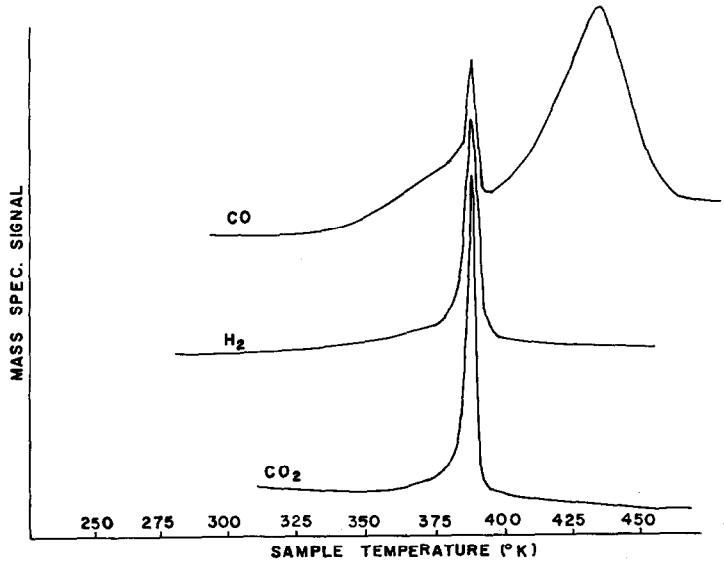

FIG. 10. Carbon dioxide, hydrogen and carbon monoxide flash desorption after 4 Langmuir exposure (through doser) of formic acid at 50°C.

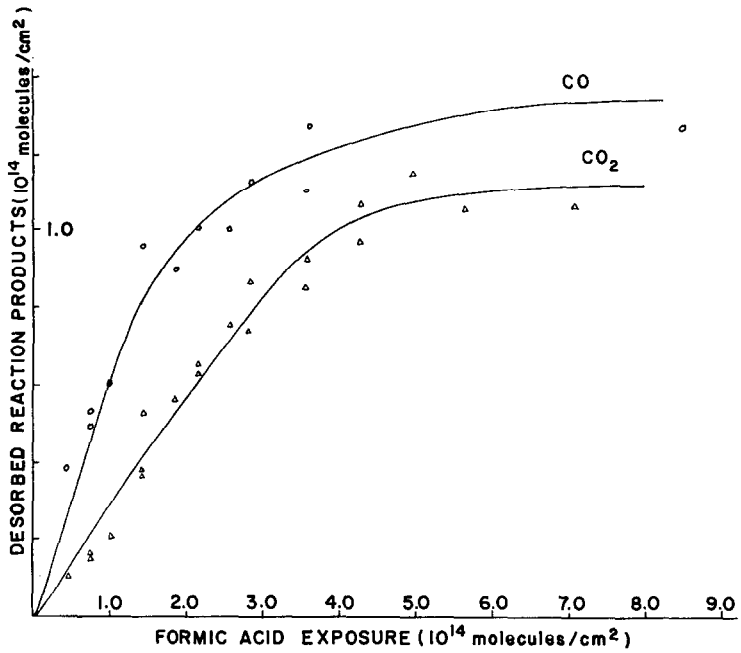

FIG. 11. Carbon dioxide, hydrogen, and carbon monoxide coverage versus formic acid exposure at 42°C.

sorption of CO from the ambient gas during HCOOH adsorption the sample was moved away from the doser so that no formic acid could directly impinge on it. After introduction of formic acid into the chamber through the syringe the H_2, CO_2, and low-temperature CO flash spectra completely disappeared and the higher temperature CO peak was reduced to less than 20% of its usual size with the crystal in this position. Repositioning the sample and trapping the formic acid in the doser line by cooling the line in a dry ice–acetone bath produced a similar effect. No H_2 and CO_2 was observed, and CO was again reduced by about 80%. Clearly, at least 80% of the second carbon monoxide flash comes from interaction of formic acid with the crystal rather than adsorption of residual CO. It was also observed that coadsorp-

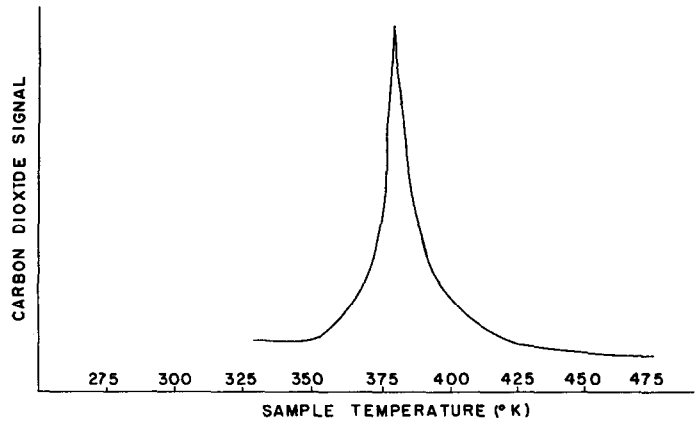

FIG. 12. Carbon dioxide flash desorption after coadsorption of formic acid and carbon monoxide.

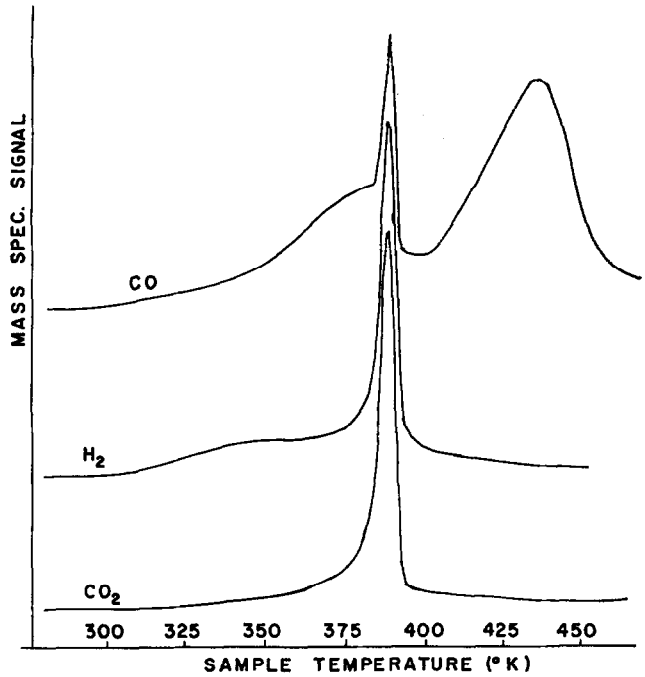

FIG. 13. Carbon dioxide, hydrogen, and carbon monoxide flash desorption after 4 Langmuir exposure (through doser) of formic acid at 28°C.

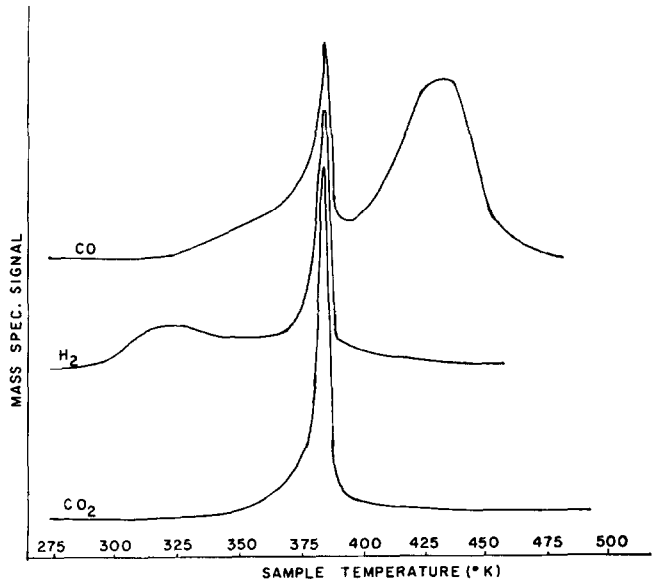

FIG. 14. Carbon dioxide, hydrogen, and carbon monoxide flash desorption after 4 Langmuir exposure (through doser) of formic acid at 3°C.

tion of CO with HCOOH yielded significant broadening of the narrow CO_2, H_2 flash peaks (see Fig. 12).

The flash spectra of formic acid adsorbed at temperatures down to 0°C were not significantly different from that at higher temperatures. Figures 13 and 14 show the CO_2, H_2 and CO flashes after formic acid adsorption at 28°C and at 3°C, respectively. With the exception of the hydrogen peak occurring at approximately 50°C the other peaks remained essentially the same. The peaks were still very narrow and occur at the same peak temperature. The hydrogen low-temperature peak increased in area with lower adsorption temperature for the same exposure. For adsorption at 53, 28, and 3°C the saturation amount of hydrogen desorbed was 3.2, 5.2, and 6.2 × 10^{14} molecules/cm^2, respectively.

In Fig. 15 are CO_2, H_2, and CO flashes for formic acid adsorption during cooling of the sample from 25°C to as low as −40°C. The narrow CO_2 and H_2 peaks have been replaced by smaller amplitude, broader peaks located at slightly lower temperatures. The CO_2 peak was decomposed into three separate peaks (69, 95, and 106°C) at high coverages. It was not possible to determine if corresponding H_2 peaks appeared, since the broad H_2 peak at 42°C partially obscured this region of the desorption spectrum. When the sample was moved away from the doser, the 42°C H_2 peak remained, though the other H_2 peak at 106°C disappeared. Thus it could not be determined if the peak at 42°C was in part due to formic acid decomposition. The ratio of CO_2 to total H_2 was approximately 1:1. The narrowing of the H_2 and CO_2 peaks was completely reversible with temperature, and after a number of broad low-temperature flashes, a flash with adsorption at 28°C, for example, yielded narrow CO_2 and H_2 peaks and no H_2 peak at a lower temperature.

The CO peak at 165°C obtained from the colder-temperature adsorption was identical to that obtained from adsorption at 50°C. The amount of CO desorbed was the same, and the temperature peak location and peak shape was unchanged. One CO peak was again identified as the CO_2 fragment. For both CO_2 and H_2 the amount desorbed after formic acid adsorption to saturation below 0°C was 5 ± 10^{14} mole-

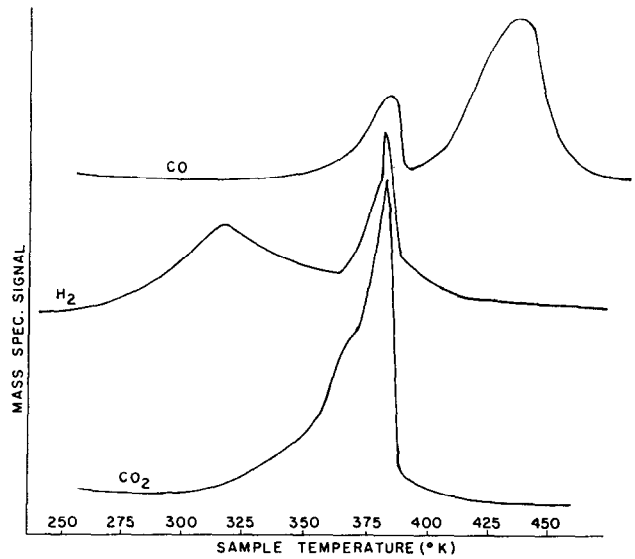

FIG. 15. Carbon dioxide, hydrogen, and carbon monoxide flash desorption after formic acid adsorption starting at 28°C and continuing while sample cooled to −30°C.

cules/cm^2. For adsorption at 28°C and above the maximum was about half this amount.

Discussion

A. Adsorption and Desorption of Hydrogen

The hydrogen flash desorption results obtained were in good agreement with other investigators. On polycrystalline nickel maximum coverages of $3.9–5.7 \times 10^{14}$ molecules/cm^2 were obtained by others (*10–12*); the value we observed was 4×10^{14} molecules/cm^2. Our observation of second order desorption kinetics was in agreement with other workers (*10, 13, 14*).

The activation energy of 25 kcal/g-mole was close to that reported for hydrogen desorption from polycrystalline nickel (*10*). Likewise for low coverages on Ni ⟨110⟩ Lapujoulade and Neil (*15*) obtained an activation energy of 20.3 kcal/g-mole. The dependence of sticking probability on surface cleanliness was observed by Gilbreath and Wilson (*9*) who obtained sticking probabilities from 0.002 on a surface with no cleaning to 0.19 at room temperature on a freshly deposited film. Our results indicated that surface carbon reduced the sticking probability. The most important observation for the purpose of this work was that hydrogen desorbed from the surface at temperatures significantly below the temperature characteristic of hydrogen desorption due to formic acid decomposition.

B. Adsorption and Desorption of Carbon Monoxide

Although earlier studies on carbon monoxide flash desorption from Ni ⟨110⟩ yielded results different from ours, more recent work using AES showed very good agreement. Degras (*16*) and Ertl and Kuppers (*17*) both observe three flash desorption peaks from Ni ⟨110⟩. Madden *et al.* (*18, 19*) observed a single first order CO flash peak at 165°C (8°C/sec heating rate) with an activation energy of 25.4 ± 1.1 kcal/g-mole and a pre-exponential factor of 10^{13} in agreement with our results. They observed two high energy peaks at approximately 380 and 530°C (17°C/sec heating rate) when the surface was exposed to oxygen or to an electron beam in the presence of CO. They attributed the higher energy flash peaks to oxygen and carbon reacting on the surface and desorbing as carbon monoxide. On the clean surface when a single flash peak was observed, Madden *et al.* observed no oxygen on the surface although they could cause a carbon increase by heating to 200°C in 2×10^{-3} Torr CO. Madden *et al.* also obtained a binding energy by LEED and Kelvin-method work function measurements of 25 kcal/g-mole for coverages above 0.7 monolayers and 30 kcal/g-mole for coverages below 0.7 monolayers. Tracy (*20*) obtained a binding energy of 31 kcal/g-mole and observed a single CO peak which desorbed below 180°C on Ni ⟨100⟩.

The near unity sticking probability we observed was also obtained by Klier *et al.* (*21*) and Tracy (*20*). Maximum coverages obtained by previous workers (*18–21*) are consistent and correspond to 1.1×10^{15} molecules/cm^2 on both the ⟨100⟩ and ⟨110⟩ surfaces. The value of 4.4×10^{14} molecules/cm^2 we obtained was consistent with the equilibrium coverages observed by Klier *et al.* due to our low adsorption pressures.

C. Adsorption and Desorption of Carbon Dioxide

It was observed that CO_2 dissociated on a nickel surface to yield adsorbed CO and oxygen. The effects of background CO were shown to be negligible and the results were similar to those observed on nickel by Khor'kov *et al.* (*22*) and on tungsten by Clavenna and Schmidt (*23*). The implications of this dissociation will be discussed in more detail with regard to the CO peaks from formic flash decomposition.

D. Formic Acid Flash Decomposition

Unlike flash desorption spectra of most gases from metal surfaces the flash peaks of hydrogen and carbon dioxide from formic acid decomposition on Ni ⟨110⟩ were extremely narrow and occurred at temperatures defined within 1°C. The desorption

temperature of hydrogen during decomposition was significantly higher than that corresponding to the desorption of hydrogen following hydrogen adsorption. Significantly, carbon dioxide desorbed after formic acid exposure although no CO_2 flash peak was observed following CO_2 exposure. Furthermore, the flash desorption peaks of CO_2 and H_2 from formic acid decomposition occurred at the same temperature with nearly identical shapes. It was apparent that the reaction pathway which yielded the sharp CO_2 and H_2 peaks did not correspond to dissociation of formic acid into CO_2 and H_2 upon adsorption. Rather, these products were apparently produced from the same reaction sequence. The value for the activation energy for formic acid decomposition of 25 kcal/mole calculated from the shift of the peak temperature with changes in heating rate agreed well with values reported in the literature (*7*, *24*, *25*). In addition the activation energy determined by holding the sample temperature at 60°C for several minutes and observing the decrease in the size of the subsequent flash peaks corresponded to approximately 25 kcal/mole.

As evidenced by the absurdly high value of the pre-exponential factor obtained from the least squares fit to the desorption rate, the peak shapes for H_2 and CO_2 did not correspond to a simple first-order decomposition of HCOOH. The striking independence of the peak temperature on the initial coverage and the shape of the decomposition trace ruled out the possibility of (a) a first order reaction with a coverage dependent activation energy (b) higher order reactions with constant activation energy, and (c) a second order reaction with a coverage dependent activation energy. In each case when the peak temperature behavior with coverage was properly accounted for, the curve shape could not be fitted, or vice versa. For example, the curve shape fitted well a first order reaction with an activation energy of the form $E = 25 + 3\theta$ kcal/g-mole, but this form of the activation energy predicted a 45°K temperature shift in the peak maximum for coverages between 4.10^{14} and 0.4×10^{14} molecules/cm^2. Generally speaking, the rate accelerated too rapidly as the reaction proceeded to be accounted for by any of the above mechanisms, while showing a coverage independent peak temperature. The most likely explanation of this behavior is that the decomposition was autocatalytic. The mechanism leading to the autocatalytic behavior is unknown at this time. Apparently the initiation step is first order in coverage, but the rate accelerates as the reaction proceeds. The general features of the flash decomposition curves are accounted for by such a kinetic process.

The decomposition of adsorbed formic acid was sensitive to the adsorption temperature. Reproducible, narrow flash desorption curves were obtained for adsorption at 25°C and above, while adsorption at temperatures less than 0°C produced much broader CO_2 and H_2 flash peaks. Adsorption at these lower temperatures also resulted in larger saturation coverages (Table 1).

The fact that formic acid oxidized the nickel surface may account for the difference for the product distribution among the results of other investigators who employed wires, evaporated films, supported metal, or metal powders in their investigations under various degrees of surface pretreatment (*1*, *4–8*, *24–27*). As shown above at low exposures CO was the predominant flash product for room temperature adsorption, and only as the exposure of formic acid was increased did CO_2 and H_2 appear in similar quantities. Previously Tamaru (*3*) observed that initial exposure of reduced nickel powders to formic acid at 100°C released hydrogen, and no CO_2 was evolved until the ratio of CO_2/H_2 adsorbed was 2/1, and Giner and Rissman (*7*) postulated that their catalysts deactivated due to oxidation of the nickel by the product CO_2. While our results on CO_2 adsorption support this postulate, we also believe that formic acid itself oxidizes the nickel surface in the absence of reducing agents in the gas phase. Furthermore, Inglis and Taylor (*2*) recently observed CO/CO_2 product ratios of 0.4 on nickel films initially, but much lower ratios were observed

TABLE 1

Desorption	T_p(°C)[a]	E_{act}[b] (kcal/mole)	Sticking probability	Maximum coverage mol/cm²
CO from CO adsorption	165	26.7	0.7 ± .2	4.4×10^{14}
H_2 from H_2 adsorption	96 (RT)	22.3	.01 ± .01	2×10^{14}
	71 (cold)	20.7		$\sim 2 \times 10^{14}$
	28 (cold)	13.0	.5 ± .1	$\sim 1.5 \times 10^{14}$
CO from formic acid adsorption	165	26.7		1.8×10^{14}
	100	22.5		2.3×10^{13}
CO_2 from formic acid adsorption	115 (RT)	23.8		1.8×10^{14}
	106 (cold)	23.3		$\sim 3 \times 10^{14}$
	95 (cold)	22.4	.9 ± .2	$\sim 2 \times 10^{14}$
	69 (cold)	20.8		$\sim 4 \times 10^{13}$
H_2 from formic acid adsorption	115 (RT)	23.8		1.8×10^{14}
	106 (cold)	23.3		$\sim 1.5 \times 10^{14}$
	50 (cold)	19.2		$\sim 4 \times 10^{14}$
CO from CO_2 adsorption	165	26.7	0.15 ± .05	1.8×10^{14}

[a] RT refers to room temperature adsorption, cold refers to adsorption below 0°C.

[b] E_{act} values are intended only to show relative activation energy differences corresponding to different T_p. These values were calculated assuming all rates were first order with a preexponential factor of 10^{13} sec^{-1}.

after more extensive exposure to formic acid. These results indicate that the product distribution shifted toward CO_2 and H_2 with surface oxidation even at low oxygen coverages.

Summary

The results of this study of formic acid decomposition on well-defined Ni ⟨110⟩ showed applicability to previous studies of the reaction in more conventional catalyst systems. It was observed that initial exposure of the surface to formic acid at room temperature resulted in the formation of CO and surface oxygen, whereas increased exposures produced CO_2 and H_2 in addition to CO. Formic acid flash decomposition was characterized by very narrow flash peaks which did not shift with exposure time prior to flashing. The behavior of these curves with coverage suggested a surface explosion mechanism for the decomposition with a slow first-order initiation step. The decomposition produced equal amounts of H_2 and CO_2. At adsorption temperatures below −30°C the characteristic decomposition peaks changed appreciably.

Acknowledgments

We gratefully acknowledge the National Science Foundation for partial support of two of us (JM, JF) through NSF traineeships throughout the course of this work. We also are indebted to the Petroleum Research Foundation of the American Chemical Society and the Center for Materials Research (NSF) for financial support. We further thank Dr. J. C. Tracy of Bell Telephone Laboratories for loan of the nickel sample employed in our studies.

References

1. Mars, P., Scholten, J. J. F., and Zwietering, P., *Advan. Catal.* **14**, 35 (1963).
2. Inglis, H. S., and Taylor, D., *Inorg. Phys. Theor.* 2905; *J. Chem. Soc.* (*A*) (1969).
3. Tamaru, K., *Trans. Faraday Soc.* **55**, 824 (1959).
4. Hirota, K., Kuwata, K., Otaki, T., and Shunkichiro, A., 2nd Inter. Congr. Catalysis Paris (1961).
5. Duell, J. J., and Robertson, A. J. B., *Trans. Faraday Soc.* **57**, 1416 (1961).
6. Nagaishkina, J. S., and Kiperman, S., *Kinet. Katal.* **6**, 1010 (1965).
7. Giner, J., and Rissman, E., *J. Catal.* **9**, 115 (1967).
8. Tamaru, K., *Trans. Faraday Soc.* **64**, 522 (1968).

9. REDHEAD, P. A., *Vacuum* **12,** 203 (1962).
10. GILBREATH, W. P., AND WILSON, D. E., *J. Vac. Sci. Technol.* **8,** 45 (1971).
11. GASSER, R. P. H., ROBERTS, K., AND STEVENS, A. J., *Trans. Faraday Soc.* **65,** 3105 (1969).
12. ELEY, D. D., AND NORTON, P. R., *Proc. Roy. Soc. (London)* **A314,** 319 (1970).
13. LAPUJOULADE, J., *Suppl. Nuovo Cimento* **V,** 433 (1967).
14. DALMAI-IMELIK, G., AND BERTOLINI, J. C., *J. Vac. Sci. Technol.* **9,** 677 (1972).
15. LAPUJOULADE, J., AND NEIL, K. S., *C. R. Acad. Sci.* **274,** 2125 (1972).
16. DEGRAS, D. A., *Suppl. Nuovo Cimento* **V,** 408 (1967).
17. ERTL, G., AND KUPPERS, J., *Surf. Sci.* **24,** 104 (1971).
18. MADDEN, H. H., AND ERTL, G., *Nederlands Tydschriff Vac. Tehnick* **10**(2) (March/April 1972).
19. MADDEN, H. H., KUPPERS, J., AND ERTL, G., "19th National Symposium of the American Vacuum Society Chicago, Ill. 3 Oct. 1972" (to be published).
20. TRACY, J. C., *J. Chem. Phys.* **56,** 2736 (1972).
21. KLIER, K., ZETTLEMOYER, A. C., AND LEIDHEISER, JR., *J. Chem. Phys.* **52,** 589 (1970).
22. KHOR'KOV, V. F., LYUBARSKII, G. D., MISCHENKO, Y. A., AND GEL'BSHTEIN, A. I., *Zh. Fiz. Khim.* **46,** 427 (1972).
23. CLAVENNA, L. R., AND SCHMIDT, L. D., *Surf. Sci.* **33,** 11 (1972).
24. CRIADO, J. M., GONZALEZ, F., AND TRILLO, J. M., *J. Catal.* **23,** 11 (1971).
25. SACHTLER, W., AND FAHRENFORT, J., "2nd International Congress on Catalysis," p. 831. Paris, 1961.
26. KISHI, K., OGAWA, T., AND HIROTA, K., *J. Catal.* **5,** 464 (1966).
27. HIROTA, K., TADAAKI, O., AND SHUNKICHIRO, A., *Zeitschriff Physikalische Chem. Neue Folge Bd* **21,** 438 (1959).